Solid-state (73) Ge NMR spectroscopy of simple organogermanes

Hanson, Margaret A.; Sutrisno, Andre; Terskikh, Victor V.; Baines, Kim M.; Huang, Yining

Publisher's version / Version de l'éditeur:
https://doi.org/10.1002/chem.201201944
Chemistry : a European Journal, 18, 43, pp. 13770-13779, 2012-09-28

Solid-State ^{73}Ge NMR Spectroscopy of Simple Organogermanes

Margaret A. Hanson[1], Andre Sutrisno[1], Victor V. Terskikh[2], Kim M. Baines[1]*, Yining Huang[1]*

[1] *Department of Chemistry, The University of Western Ontario, London, Ontario, Canada* N6A 5B7

[2] *Measurement Science and Standards, National Research Council Canada, Ottawa, Ontario, Canada K1A 0R6*

Abstract

Germanium-73 is an extremely challenging nucleus to examine by NMR spectroscopy due to its unfavourable NMR properties. Through the use of an ultrahigh (21.1 T) magnetic field, a systematic study of a series of simple organogermanes was carried out. In those cases where X-ray structural data were available, correlations were drawn between the NMR parameters and structural metrics. These data were combined with DFT calculations to obtain insight into the structures of several compounds with unknown crystal structures.

Introduction

^{29}Si nuclear magnetic resonance (NMR) spectroscopy has proven to be an invaluable tool for the structural characterization of organosilicon compounds, both in liquid and solid states, offering insight beyond that available from ^{1}H and ^{13}C NMR spectroscopy.[1] Of particular utility is the ability to examine the actual nucleus of interest, Si, rather than relying on indirect information via organic substituents. Obtaining comparable information for germanium compounds is considerably more difficult due to the unfavourable properties of ^{73}Ge, the only NMR-active isotope of germanium.[2] While ^{29}Si is a spin-1/2 nucleus, ^{73}Ge is quadrupolar, with

a spin of 9/2 and a moderately large quadrupolar moment of -19.6 fm^2,[3] leading to broad lines in the absence of ideal spherical symmetry. While the natural abundances of these nuclei are similar (4.5% for ^{29}Si and 7.7% for ^{73}Ge) the greatest challenge arises from the inherent lack of sensitivity due to the gyromagnetic ratio of ^{73}Ge, which, at 0.9332×10^7 $radT^{-1}s^{-1}$, is among the lowest in the periodic table.

In recent years, there have been several developments that improved NMR accessibility of low γ nuclei. The increasing availability of ultrahigh field NMR spectrometers is particularly promising for ^{73}Ge NMR spectroscopy. Operating at very high magnetic field greatly enhances the sensitivity of low gyromagnetic ratio nuclei. Solid-state NMR (SSNMR) line broadening due to quadrupolar interactions is inversely proportional to the magnetic field strength, leading to narrower lines at higher fields. Additionally, performing NMR experiments at very high magnetic field allows the chemical shielding (CS) tensor, which provides invaluable information on bonding and structure, to be measured more accurately since the effect of chemical shielding anisotropy (CSA) on lineshape is directly proportional to field strength. At lower fields, the quadrupolar interaction tends to completely dominate over the CSA, while ultrahigh fields offer the potential to observe both, and thus, obtain additional structural insight. Sensitivity-enhancement techniques such as Quadrupolar Carr-Purcell-Meiboom-Gill (QCPMG)[4] and related pulse sequences[5] have proven valuable in increasing the signal-to-noise ratio of broad quadrupolar patterns. Recently, the incorporation of WURST pulses has further improved the excitation bandwidth of the QCPMG technique.[5b] As ^{73}Ge spectra are generally expected to be broad with poor signal-to-noise ratios under favourable conditions, WURST-QCPMG has the potential to significantly ease their acquisition.

Due to the inherent challenges, ^{73}Ge SSNMR studies have, so far, been very limited. One of the earliest solid-state ^{73}Ge NMR investigations involved single crystals of elemental germanium.[6] The large quadrupole moment of the ^{73}Ge nucleus was used to detect disorder induced by changes in the isotopic makeup of the single crystal. The first investigation of a substituted organogermanium center involved the symmetrically substituted $GePh_4$ and $Ge(CH_2Ph)_4$ under magic angle spinning (MAS) conditions.[7] While the former compound gave a single sharp signal in a reasonable time-frame; the latter compound required extended acquisition times to acquire only a broad, featureless signal. The difference was attributed to the slightly different Ge-C bond lengths causing deviation from ideal tetrahedral symmetry in $Ge(CH_2Ph)_4$. Even with extended experiment times, the lineshapes were not sufficiently resolved to extract quadrupolar parameters, and thus, only a linewidth at half height and a peak maximum were reported. This report was followed in 2004 with a study of hexacoordinate germanes.[8] While several systems with differing ligands were examined, only signals from the symmetrical systems were observed in the solid state. A third study of organogermanes returned to tetracoordinate systems.[9] The majority of the compounds studied were once again symmetrically substituted, but a few lower symmetry compounds were also included in the study. In general, the tetraaryl systems had distorted S_4 symmetry, resulting in broader lines than were observed for $GePh_4$. Thus, longer experiment times were required, sometimes on the order of weeks. Although the less symmetrical systems generally did not give rise to signals, the ^{73}Ge SSNMR spectra of $Ph_2Ge(p\text{-}C_6H_4Me)_2$ and $Ph_3Ge(p\text{-}C_6H_4Me)$ revealed broad signals. This was the first indication that it might be feasible to study lower symmetry systems, though the long experiment times still presented a significant challenge at that time.

Due to the many unfavourable magnetic resonance properties of ^{73}Ge, ultrahigh magnetic fields are expected to be particularly beneficial. Germanium dioxide was the first material studied by ^{73}Ge SSNMR spectroscopy using a 21.1 T magnet.[10] This work was later expanded to several different polymorphs of GeO_2.[11] Through the use of the QCPMG pulse sequence at ultrahigh field, it was possible to obtain sufficiently defined lineshapes to extract the quadrupolar parameters via spectral simulation. A comprehensive study of germanium oxide materials with different local structures about germanium, coordination environments and countercations was then conducted to establish trends in the ^{73}Ge NMR parameters.[12] In general, crystalline materials gave well-defined signals, while vitreous materials gave broad, featureless spectra. A similar situation was observed in the case of germanium selenide glasses,[13] yielding only an average environment around germanium rather than the full range of structural information potentially available from SSNMR spectroscopy. Germanium SSNMR was also used to provide insight into the diverse structural environments in germanium di- and tetrahalides.[14] In a recent communication, we examined $GePh_4$ and $GeCl_2$·dioxane at ultrahigh field.[15] These two compounds are representative of the two extremes of ^{73}Ge SSNMR spectral data: $GeCl_2$·dioxane exhibited an extremely broad spectrum with a quadrupolar coupling constant (C_Q) of 44 MHz, the largest observed for ^{73}Ge by NMR spectroscopy to date. $GePh_4$, on the other hand, exhibited a very small quadrupolar interaction, allowing for the first direct observation of CSA in a ^{73}Ge system.

In this work, we report a systematic investigation of the potential of ^{73}Ge SSNMR spectroscopy by examining simple organogermanium compounds with a range of substituents (Figure 1). The majority of these compounds are symmetrical tetra-substituted organogermanes. Specifically, we have investigated the ^{73}Ge SSNMR spectra of tetraarylgermanes including Ge(*p*-

Me-$C_6H_4)_4$ (**1**), Ge(*p*-MeO-$C_6H_4)_4$ (**2**) and $GePh_4$ (**3**). While $GePh_4$ exhibits near perfect T_d symmetry, Ge(*p*-Me-$C_6H_4)_4$[16] exhibits a range of bond lengths and angles, which offers the potential to examine the sensitivity of quadrupolar and CSA parameters to small variations in structure. We also examined three other tetra-substituted germanes: tetrabenzylgermane[7] (**4**), tetra(*tert*-butoxy)germane (**5**) and tetrakis(trimethylsilyl)germane (**6**). These are prototypical examples of tetraalkyl, tetraalkoxy and tetrasilylgermanes, respectively, which will allow an investigation into the effect of different chemical environments on ^{73}Ge SSNMR parameters. While sites of tetrahedral symmetry are the most amenable to ^{73}Ge SSNMR spectroscopy, systems of chemical interest seldom meet this criterion. To determine the scope of the technique, our study included three less symmetrical germanes: dimesitylgermane (**7**), trimesitylgermane (**8**) and bis(trimethylsilyl)dimesitylgermane (**9**). Of the mesitylgermanes, only Mes_3GeH has a known, albeit disordered, crystal structure.[17] In recent years, there has been an interest in using solid-state NMR spectroscopy as a complement to X-ray diffraction for structure determination.[18] Using a combination of ^{73}Ge SSNMR trends observed in the tetra-substituted systems with known crystal structures and computational modelling, we were able to obtain partial structural information on germanes **7-9**.

Results and Discussion

Tetraorganogermanes

We first examined three tetraarylgermanes including Ge(*p*-Me-$C_6H_4)_4$, Ge(*p*-MeO-$C_6H_4)_4$, $GePh_4$ and tetrabenzylgermane. The reasons for choosing these compounds are the following: (1) in all these compounds, Ge is tetrahedrally bound to four identical ligands, which should result in a reasonably small C_Q, making detection of a ^{73}Ge signal more feasible. (2) The crystal structures of these compounds are known, which allows us to examine the sensitivity of

^{73}Ge SSNMR parameters to the local environment. (3) For each compound, there is only one distinct Ge site in the unit cell, simplifying the spectral interpretation.

Figure 2 shows the MAS and static spectra of **1-4** obtained at 21.1 T. The NMR tensor parameters extracted from spectral simulations are given in Table 1. The MAS spectrum of Ge(*p*-Me-$C_6H_4)_4$ (Figure 2A) exhibits a lineshape which is typical of half-integer quadrupolar nuclei experiencing residual second-order quadrupolar interaction under MAS conditions. The spectrum can be very well simulated by a single ^{73}Ge signal with C_Q = 3.9 MHz, η_Q = 0.7 and δ_{iso} = -25 ppm. Observing one resonance is consistent with the crystal structure of this compound. The relatively small C_Q is indicative of a rather symmetric local environment around Ge. Indeed, an inspection of the crystal structure reveals that the variations in the Ge–C bond lengths are very small (within 0.016 Å). The deviations of the C–Ge–C bond angles from ideal tetrahedral angles are also rather small (i.e., the largest deviation is only ~2°). The value of the asymmetry parameter is closer to one than zero, suggesting that the EFG is non-axial symmetric, which is consistent with the low Ge site symmetry (C_1). The ^{73}Ge isotropic shift of -25 ppm is in reasonable agreement with the previously reported value of -32.4 ppm;[9] however, Takeuchi did not report lineshape information beyond the breadth of the line.[9] The static ^{73}Ge spectrum of Ge(*p*-Me-$C_6H_4)_4$ (Figure 2B) acquired at 21.1 T can be fit using the same set of EFG tensor parameters with the inclusion of a small CSA (Ω = 30 and κ = 0.2). The individual contributions from the EFG and the CSA are shown in Figure S1A. It is clear the second-order quadrupolar interaction dominates the spectrum. The presence of a small CSA is ambiguous at this point since the static spectrum was only acquired at one field (an attempt to record a static spectrum at 9.4 T was unsuccessful); however, it was later confirmed by DFT calculations (see below).

The MAS spectrum of Ge(p-MeO-C_6H_4)$_4$ (**2**) is shown in Figure 2C. The signal-to-noise (S/N) ratio is still rather poor after 17 hours of acquisition. The spectral breadth is larger than that of Ge(p-Me-C_6H_4)$_4$. Simulations yielded the following EFG parameters: C_Q = 5.0 MHz, η_Q = 0.9 and δ_{iso} = -20 ppm. The larger C_Q in Ge(p-Me-C_6H_4)$_4$ suggests that the distortion of local Ge geometric environment from tetrahedral symmetry must be larger compared to that in Ge(p-Me-C_6H_4)$_4$. As the X-ray structure of Ge(p-MeO-C_6H_4)$_4$ was not reported, single crystals were grown (Table S2). As expected, the structure is a distorted tetrahedron, with C–Ge–C angles ranging from 107.4(1) to 111.2(1)°, Ge-C bond lengths ranging from 1.940(3) to 1.950(3) Å and there is no specific site symmetry at the germanium center (Table S3). The fact that the Ge–C distances found in Ge(p-MeO-C_6H_4)$_4$ are slightly shorter than those in Ge(p-Me-C_6H_4)$_4$ accounts for the larger C_Q of **2**. The value of η_Q=0.9, is consistent with the low Ge site symmetry. The isotropic shift found for Ge(p-MeO-C_6H_4)$_4$ (-20 ppm) lies between the reported solution state values of -11.3 ppm reported by Takeuchi[9] and that reported by Yoder (-27.1 ppm) .[19] We were unable to acquire a static spectrum at 21.1 T in a reasonable period of time, excluding the possibility of measuring the CSA.

For $GePh_4$ (**3**), preliminary ^{73}Ge NMR results were reported in a communication.[15] The MAS spectrum of **3** (Figure 2D) exhibits a very sharp single line, suggesting the quadrupolar interaction experienced by the Ge in this compound is very small. The EFG parameters determined from the static spectrum at 21.1 T were $C_Q \leq 0.5$ MHz and δ_{iso} = -30 ppm. The very small, but non-zero C_Q can be attributed to the high site symmetry at Ge. The striking feature of the static spectrum of $GePh_4$ (Figure 2E) is that the lineshape of the central transition is clearly dominated by a small but measurable CSA with Ω = 30 and κ = -1. The skew value is consistent with the axial site symmetry. The reason why such a small CSA can be observed directly and

accurately is the combination of a very small EFG and performing the NMR measurement at ultrahigh magnetic field because the effect second-order quadrupolar interaction on linewidth is scaled down linearly with magnetic field and the effect of CSA increases proportional to the strength of the field applied.

The MAS spectrum of $Ge(CH_2Ph)_4$ (**4**) (Figure 2F) shows a single peak. Although very narrow (full width at half height (FWHH) = 400 Hz), the signal does exhibit a typical quadrupolar line-shape. The simulations yielded C_Q = 2.5 MHz, η_Q = 1.0 and δ_{iso} = 4.5 ppm. The asymmetry parameter (η_Q = 1.0) indicates an absence of axial symmetry. This is consistent with the molecular structure in the solid state, where the Ge center is located at a general position with no specific site symmetry.[20] The Ge–C bond lengths in $Ge(CH_2Ph)_4$ range from 1.946(6) to 1.973(6) Å and the C–Ge–C angles range from 106.9(3) to 110.7(3)°. The distortion from ideal tetrahedral local geometry results in a notable EFG. The C_Q value of $Ge(CH_2Ph)_4$ is smaller than in both $Ge(p\text{-}Me\text{-}C_6H_4)_4$ and $Ge(p\text{-}MeO\text{-}C_6H_4)_4$, which can be rationalized by the fact that the Ge-C bond distances in $Ge(CH_2Ph)_4$ are longer than those in $Ge(p\text{-}Me\text{-}C_6H_4)_4$ and $Ge(p\text{-}MeO\text{-}C_6H_4)_4$ while the symmetry is similar. The static spectrum of $Ge(CH_2Ph)_4$ (Figure 2G) at 21.1 T exhibits a complex lineshape suggesting the presence of CSA. The simulation of the static spectrum indeed reveals the presence of the CSA with Ω = 60 ppm and κ = 0.9, confirming that the observed spectrum contains contributions from both the quadrupolar and chemical shift interactions. Although we were not able to obtain the static spectrum at a second (lower) field due to the low sensitivity, in this particular case, the existence of CSA is unambiguous. As shown in Figure S1B, the observed lineshape at 21.1 T definitely cannot be reproduced by using only the EFG parameters extracted from the MAS spectrum. Thus, $Ge(CH_2Ph)_4$ is another example where the CSA is directly and unambiguously observed by experiment. The span is twice of that

$GePh_4$ and the skew ($\kappa = 0.9$) is consistent with the non-axially symmetric environment around germanium observed in the molecular structure of the germane in the solid state.[20]

To better understand the experimental results and to rationalize these results in light of available structural information, we carried out computational NMR studies. Previous computational studies of ^{73}Ge NMR parameters[11-12, 15, 21] have made use of the plane wave pseudopotential method in the CASTEP program, which has proven to be an excellent method to predict NMR tensor parameters of crystalline solids.[22] However, the large (> 1000 Å^3) volumes of the unit cells of the structures in this study[16, 20] made this method practically unfeasible with available computational resources. Since the solids of all the compounds in this study contain discrete molecules rather than infinite framework materials, it is feasible to investigate these systems using first principles calculations in Gaussian 09.[23] In order to optimize the computational methodology, we tested the suitability of various computational methods and basis sets for predicting ^{73}Ge NMR tensor parameters. We first performed the calculations on Ge(*p*-Me-C_6H_4)$_4$ using restricted Hartree-Fock (RHF) and density functional theory (DFT) with several different functionals (B3LYP,[24] TPSSTPSS,[25] PBE1PBE[26]) and two basis sets (6-31G*, 6-311+G**). As the X-ray structure of Ge(*p*-Me-C_6H_4)$_4$[16] did not include hydrogen atoms, their assumed positions were added and optimized at the TPSSTPSS/6-31G* level. The results are summarized in Table 2. Generally, when using the smaller 6-31G* basis set, the calculations significantly underestimated C_Q and overestimated the CS parameter (both span and skew) of Ge(*p*-Me-C_6H_4)$_4$ (Table 2, entries 1-4), regardless the method and functional used. The agreements between the calculated and measured C_Q improve significantly when using a larger basis set of 6-311+G** (Table 2, entries 5-8). The calculations consistently yielded a small CSA ranging from 32 to 35 ppm independent of the method and the functional utilized, which is

important given that the experimental results were obtained only at one magnetic field. Since the relatively recent TPSSTPSS[25] functional gave accuracies comparable to the other model chemistries employed in approximately half the computational time, this functional was utilized in this work as the preferred functional for subsequent calculations. The results of the calculations on compound **2-4** are summarized in Table 1. Figure 3 shows that the agreement between experiment and theory for C_Q of **1-4** is reasonably good.

Previous studies suggested that the magnitude of C_Q (^{73}Ge) of germanium oxides and halides can be related to the tetrahedral and octahedral distortion.[12] As we are interested in ^{73}Ge SSNMR spectroscopy as a diagnostic tool for the structural characterization of organogermanium compounds, we also looked for correlations between the NMR parameters and structural features. In this work, the quadrupolar coupling constant was found to correlate reasonably to the average Ge–C bond length as determined by X-ray crystallography within sets of compounds with similar symmetries, with longer bonds yielding smaller quadrupolar interactions (hence small C_Q) in three tetraarylgermanes (Figure 4A). The experimental value observed for $Ge(CH_2Ph)_4$ did not fit the observed trend. However, $Ge(CH_2Ph)_4$ was the only case in which the calculated C_Q was negative. While it is not possible to determine the sign of C_Q from an NMR experiment, if it is assumed to be the same as the theoretical case, this point also becomes consistent with the larger trend (Figure 4A).

The influence of the magnitude of the C–Ge–C bond angles was also examined. The average angle did not correlate directly to any EFG parameter; however, the overall distortion from ideal tetrahedral angles, as quantified by the distortion index[27] defined by $DI=\sum(|\theta - \theta_i|/6\ \theta_i)$ where θ is the bond angle and θ_i is the ideal tetrahedral bond angle, 109.5°, was found to correlate with C_Q. A greater distortion from ideal tetrahedral symmetry led to larger magnitudes

of C_Q in a linear fashion (Figure 4B). Finally, trends in the NMR parameters of tetraarylgermanes were examined in terms of pure electronic effects. Using standard Hammett constants, a linear correlation was found (Figure 4C), with more electron-rich germanes possessing larger C_Qs. The isotropic shifts of these compounds also correlate linearly in these compounds, with substituents with a more negative σ value having a larger deshielding effect at germanium (Figure 4D).

Due to the limited number of data points in this series, we further explored the validity of these empirical trends computationally. Starting from the experimental geometry of $GePh_4$, one structural metric was systematically distorted. Compression of one Ge–C bond length led to an increase in the calculated value of C_Q (Figure 5A), in keeping with the trend observed experimentally (Figure 4A). Elongation of the same bond beyond the experimental value of 1.95 Å led to an increase in the magnitude of C_Q as the sign became negative. There did not appear to be any correlation between the bond length and the calculated value of η_Q. The effect of the magnitude of the C–Ge–C bond angles on C_Q and η_Q was also examined. A single angle was systematically varied. Consistent with experimental observations, the size of the angle did not correlate to any calculated parameters; however, when the effect of the angles was examined in terms of distortion from T_d symmetry using distortion index as a parameter, there was a linear correlation to C_Q (Figure 5B). There was, once again, no clear trend in η_Q. Overall, the theoretical calculations confirm the trends established using empirical correlations.

Mesitylgermanes

Mes_2GeH_2 (**7**) and Mes_3GeH (**8**) represent two systems whose structures are either unknown or poorly described. At 21.1 T, the ^{73}Ge MAS spectra (Figure 6A, C) of these two compounds with seemingly very asymmetric Ge environments exhibit surprisingly narrow signals (FWHH = 500 Hz and 700 Hz for Mes_2GeH_2 and Mes_3GeH, respectively) rather than the

expected broad EFG-dominated pattern. The more shielded shift in Mes_2GeH_2 indicates that replacing aryl groups with hydride ligand increases the shielding at the germanium center, consistent with the established trends in ^{29}Si NMR spectroscopy.[1]

The EFG parameters of Mes_2GeH_2 extracted from spectral simulation are $\eta_Q = 0.7$ and $C_Q = 2.3$ MHz. The value of C_Q is much smaller than those of the tetraarylgermanes examined in this study (Table 1). While the C_Q of Mes_3GeH (2.9 MHz) is larger than that of Mes_2GeH_2, it is smaller than those of the *p*-substituted tetraarylgermanes **1** and **2**. The asymmetry parameter for Mes_3GeH is 0.7, indicating an absence of axial symmetry despite the possibility of a C_3 axis through the Ge–H bond. The static spectrum of Mes_2GeH_2 (Figure 6B) at 21.1 T cannot be reproduced by using only the EFG parameters obtained from the MAS spectrum alone. In fact, Figure 6 shows that the static spectrum is most likely dominated by the CSA interaction. Mes_2GeH_2 has a span of approximately 100 ppm, the largest ^{73}Ge CSA observed to date. The effect of CSA on the Mes_3GeH spectrum is more subtle, but as shown in Figure 6D, it is still required in order to better simulate the static lineshape. The span ($\Omega = 50$) of the CSA tensor of **8** is smaller than that of Mes_2GeH_2. Mes_2GeH_2 and Mes_3GeH have skew values (-0.6 in both cases) indicating an absence of axial symmetry, consistent with the EFG observations.

A disordered crystal structure was reported for Mes_3GeH.[17] Using the structural parameters reported in the literature, the DFT calculations predicted the following NMR parameters: $C_Q = 23.3$ MHz, $\eta_Q = 0.17$. The powder pattern, predicted based on the reported molecular structure, is dominated by the EFG and remarkably different from the experimentally measured spectrum (Figure S2), implying that the true molecular geometry in the solid state at room temperature differs from the one reported in the literature. The difference is unlikely to be due to extensive molecular motion, as the large size of the mesityl groups does not allow for

rapid rotation even in solution. To understand why Mes_3GeH, a compound with a seemingly asymmetric environment around Ge, has a very small C_Q and to gain information on its true crystal structure, we carried out computational modelling to explore the effect of bond length and C-Ge-C angle on C_Q. The results are shown in Figure 7. The structure of Mes_3GeH was first geometry optimized in Gaussian 09, yielding a structure with a C_Q value of 4.6 MHz. While this was considerably better agreement with experiment, it still was greater than the measured value. The structural metrics were varied systematically in an attempt to obtain better agreement. The optimized structure featured three equal C–Ge–C angles. Any slight alteration of one angle caused C_Q to increase dramatically to approximately 30 MHz (Figure 7A). Thus, the C–Ge–C angles were left unaltered in the final proposed structure. The Ge–H bond length had a substantial (180 MHz/Å) effect on the calculated C_Q (Figure 7B). Changing this metric from the optimized value rapidly increased C_Q well above the experimental value, and thus, the optimized value was also retained in the final structure. The most important variable for the determination of the final proposed structure was, thus, the Ge–C bond lengths. To minimize the number of variables, initial calculations altered all Ge–C bonds simultaneously. This yielded a linear trend, with a minimum value less than experiment (Figure 7C). There were two possible bond lengths that gave calculated values consistent with experiment: 1.97 Å (C_Q = 2.7 MHz) and 2.00 Å (C_Q = 3.1 MHz). In view of the large size of the mesityl group, the longer Ge-C distance appears to be more plausible and this is also consistent with the average Ge-C bond (2.045 Å) reported in the disordered structure.[17] The calculated η_Q value (η_Q=0) at the same geometry does not correspond to experimental one (0.7), suggesting that the C_3 symmetry imposed on the model does not exist in the actual structure. Indeed, the inequivalence of the three mesityl groups is supported by the ^{13}C CPMAS SSNMR spectrum of Mes_3GeH which exhibits multiple resonances for each chemically distinct carbon of mesityl group (Figure 8A). The fact that

changing one C–Ge–C bond angle from the optimized geometry by even half of a degree caused the calculated C_Q to increase by approximately 30 MHz suggests that the deviation from axial symmetry is more likely due to non-equivalent bond lengths rather than angular distortion. When only one bond length is altered, the correlation to C_Q remains linear (Figure 7D) while the value of η_Q rapidly rises from zero to more reasonable values (Figure S3). Taking all the factors into consideration, the following structural parameters: Ge–H= 1.55 Å; ∠ C–Ge–C = 115° x 3; Ge–C_1= 1.99 Å and Ge–C_2 = 2.00 Å x 2 lead to C_Q = 2.7 MHz and η_Q=0.8. The final proposed structure represents one of many possibilities as multiple combinations of Ge-C bond lengths would yield similar C_Q values. It was not possible to further refine the structure without additional constraints.

The overall structure adopts a propeller geometry due to the steric effect of the *ortho* methyl groups on the mesityl substituents. In the absence of such an interaction, all six ortho carbons would lie in a single plane, leading to a C_{ipso}–Ge–C_{ipso}–C_{ortho} dihedral angle of 30°; however, when the rings rotate to minimize the methyl-methyl interactions (Figure 9), one angle (α) becomes smaller while the other (β) becomes larger. These angles appear three times within the structure. The overall distortion can be described in terms of the average $\varphi = 0.5[(\alpha+30)+(\beta-30)]$, where α and β are the average values of the angles in a single structure. In the proposed structure, as determined by ^{73}Ge SSNMR spectroscopy and computational modeling, φ is 32°, indicating that the structure is less twisted than was observed in the X-ray structure (φ = 42°). It is possible that this difference arises from slight structural changes at room temperature when compared to the low temperature at which the X-ray data were collected.

A similar approach was used to approximate the structure of Mes_2GeH_2 whose crystal structure is not known. When using the geometry optimized structure, the calculated quadrupolar

coupling constant for Mes_2GeH_2 was found to be 5.4 MHz, somewhat greater than the experimental value of 2.3 MHz. As the Ge–C bond length has already been shown to considerably affect the largest EFG component, the Ge–C bond lengths of Mes_2GeH_2 were altered in an effort to approximate the experimental parameters (Figure S4A). Elongation of the two Ge–C bonds led to a minimum value of C_Q of 2.2 MHz at a Ge–C bond length of 1.97 Å (geometry optimized value: 1.95 Å). The Ge–H bond length once again had a dramatic (180 MHz/Å) effect on the value of C_Q (Figure S4B). Altering the Ge–H bond length rapidly increased C_Q well beyond the experimental value, and thus, it was left at the optimized value. While the H–Ge–H angle had a negligible impact (Figure S4C), the C–Ge–C angle had a small but noticeable effect (Figure S4D). However, the optimized value proved to give the best agreement with experiment. Thus, we predict the molecular structure of Mes_2GeH_2 to have an average Ge–C bond length of 1.97 Å and a C–Ge–C bond angle of 113°. The span of the CSA tensor at the final geometry was calculated to be 124 ppm, in reasonable agreement with the experimental value of 100 ppm (Table 1). The ^{13}C CPMAS SSNMR spectrum (Figure 8B) shows very sharp resonances for two distinct *ortho* methyl groups and one *para* methyl group as well as a total of five aromatic carbons. This most likely arises from the carbons within the individual mesityl groups being crystallographically inequivalent while two mesityl groups are likely related by either a C_2 axis or a mirror plan, making them equivalent or very nearly so.

Tetrakis(trimethylsilyl)germane and tetra(tert-butoxy)germane

For $Ge(SiMe_3)_4$ (**6**), the MAS and static spectra (Figure 10C,D) acquired at 21.1 T both exhibit sharp single resonances (FWHH ~65 Hz), indicating that the Ge experiences neither quadrupolar nor CSA interactions. Such observations are consistent with its crystal structure,[28] which shows that the molecule adopts an ideal T_d symmetry. Furthermore, the ^{13}C CPMAS

SSNMR spectrum of **6** (Figure 8C) shows a single sharp resonance, suggesting that, much like in $Si(SiMe_3)_4$,[29] $Ge(SiMe_3)_4$ undergoes rapid isotropic motion about a fixed center of mass, leading to a solution-like environment around germanium, and thus, a lack of effect on lineshape from CSA and EFG.

Similar to $Ge(SiMe_3)_4$, both MAS and static spectra of $Ge(OtBu)_4$ (**5**) (Figure 10A,B) show a relatively narrow and symmetric resonance (FWHH = 2 kHz). The fact that the FWHHs of the static and MAS spectra of **5** are nearly identical supports the absence of an observable electric field gradient and CSA as the molecules likely undergo fast isotropic reorientation in solids. While there is no known crystal structure for $Ge(OtBu)_4$, some information can be obtained from solid-state ^{73}Ge and ^{13}C NMR spectral parameters. The Ge spectra indicate that there is only one unique Ge site with a high symmetry in the unit cell. The ^{13}C spectrum of **5** exhibits one sharp resonance at 32 ppm assigned to the methyl groups and one at 75 ppm assigned to the quaternary carbon based on the chemical shifts (Figure 8D). The observation of a single sharp ^{13}C signal assigned to the quaternary carbons suggests that the four O*t*Bu groups are identical, further confirming the high symmetry of $Ge(OtBu)_4$. The twelve methyl groups only produces one sharp signal, indicating rapid rotation of the *t*-butyl groups around the O–C bond leading to high molecular symmetry on the NMR time scale at room temperature.

Dimesitylbis(trimethylsilyl)germane

Replacing two of the trimethylsilyl ligands in $Ge(SiMe_3)_4$ with mesityl groups changes the appearance of the static ^{73}Ge SSNMR spectrum in a dramatic fashion. The signal is so wide that the WURST-QCPMG method had to be used to acquire the spectrum. Rather than a single narrow line, $Mes_2Ge(SiMe_3)_2$ exhibits the broadest signal of any observed in this study with a breadth greater than 200 kHz (Figure 10E). The magnitude of the quadrupolar coupling constant

(C_Q = 24.7 MHz) is very large, which is consistent with the large EFG expected for a Ge local environment significantly deviating from spherical symmetry. The asymmetry parameter (η_Q = 0.6) indicates the absence of axial symmetry. While the quadrupolar interactions of the two dimesityl compounds are quite different, the isotropic shift (-173 ppm) is similar to that observed for Mes_2GeH_2. The inclusion of CSA was not required for spectral simulation, due to the magnitude of the quadrupolar interaction dominating the spectrum. A CSA of 30-100 ppm such as observed in the compounds examined in this study would not have an observable impact on the overall lineshape. Due to the extreme breadth of the static spectrum, MAS experiments were not performed.

Since the crystal structure of $Mes_2Ge(SiMe_3)_2$ is not known, computational modelling was conducted to gain information on the molecular geometry in the solid-state. The experimental C_Q (24.7 MHz) was somewhat underestimated at the Gaussian optimized geometry (19.3 MHz), though it did give reasonable agreement with η_Q (experimental = 0.6, calculated = 0.5). The Ge–C and Ge–Si bond distances and angles were systematically varied to explore their effect on C_Q. As previously observed, the Ge–C bond length continued to have a dramatic (121 MHz/Å) effect on the magnitude of calculated C_Q (Figure S5A); however, elongation of the germanium-silicon bonds also caused a non-negligible (-85 MHz/Å) decrease in C_Q (Figure S5B). The C–Ge–C (Figure S5C) bond angle caused small (-0.5 MHz/°) but systematic changes in the calculated C_Q. While the effect of the Si–Ge–Si (Figure S5D) angle was also systematic, the overall impact was negligible (-0.06 MHz/°). In $Mes_2Ge(SiMe_3)_2$, the predicted η_Q correlated linearly to both the Ge-C (Figure S6A) and the Ge-Si (Figure S6B) bond lengths, providing an additional constraint to approximate the structure. The C–Ge–C angle also had a small effect on the overall EFG tensor (Figure S6C), while the effect of the Si–Ge–Si angle was again negligible

(Figure S6D). The final geometry tested was, thus, selected to give a larger C_Q than calculated for the optimized geometry while keeping η_Q close to its experimental value. The final geometry was determined by varying the Ge–C bond length to raise the calculated value of C_Q to the highest value possible without raising η_Q above its experimental value. C_Q was then further adjusted by contraction of the Ge–Si bond until the same limit was reached. Finally, fine adjustments to the calculated value of C_Q were made by altering the C–Ge–C and Si–Ge–Si angles. With a Ge–C bond length of 2.01 Å, a Ge–Si bond length of 2.4 Å, a C–Ge–C bond angle of 104° and a Si–Ge–Si bond angle of 105°, the quadrupolar parameters were calculated to be C_Q = 24.5 MHz and η_Q =0.5, which is within experimental error of the observed values (Table 1). While both bond lengths (Ge-C or Ge-Si) were kept the same to minimize the number of variables, the ^{13}C CPMAS SSNMR spectrum of **9** indicates that neither the mesityl groups nor the trimethylsilyl groups are actually equivalent to each other (Figure 8E). The bond lengths obtained in this manner thus represent a predicted *average* value. One can further adjust the bond lengths to make two mesityl groups inequivalent (one of such possibility, with Ge–C bond lengths of 2.01 and 2.005 Å, is listed in Table 1). Since there are many possible combinations, the structure was not refined further.

Conclusion

Obtaining useful ^{73}Ge SSNMR spectra of organogermanium compounds for structural analyses has been traditionally very difficult due to the extremely low sensitivity. The present work demonstrates that ^{73}Ge SSNMR spectra in favourable cases can now be obtained at ultrahigh magnetic field. We have shown that for the compounds with a known crystal structure, the ^{73}Ge MAS and static spectral parameters are very sensitive to the Ge local environment. The

^{73}Ge NMR tensor values were correlated with the structural parameters. The combination of ^{73}Ge SSNMR data and computational modelling provides insight into the local geometry around Ge for organogermanes of unknown or poorly described structures. ^{73}Ge SSNMR spectroscopy at ultrahigh magnetic field is a promising method for the characterization of organogermanium compounds.

Experimental

Materials

Tetrabenzylgermane,[30] Ge(*p*-Me-C_6H_4)$_4$,[16] Ge(*p*-MeO-C_6H_4)$_4$,[9] tetra(*tert*-butoxy)germane,[31] tetrakis(trimethylsilyl)germane,[32] dimesitylgermane,[33] trimesitylgermane[17] and dimesitylbis(trimethylsilyl)germane[34] were prepared according to literature procedures. X-ray quality single crystals of Ge(*p*-MeO-C_6H_4)$_4$ were grown from dichloromethane/isopropanol.

Solid-State NMR Spectroscopy

^{73}Ge SSNMR spectra were acquired on a Bruker Avance 900 MHz spectrometer at the *National Ultrahigh Field NMR Facility for Solids* (www.nmr900.ca). Experimental setup and pulse calibrations were performed on neat $GeCl_4$. Chemical shift referencing was also performed relative to the same sample of $GeCl_4$ (30.9 ppm relative to $GeMe_4$ at 0 ppm). Magic-angle spinning experiments were performed on a 7 mm single channel low gamma MAS probe. A one-pulse experiment was performed using a solid 90° pulse with a 1-2 second recycle delay, spinning at 4-5 kHz. Static experiments with proton decoupling were performed on a home built 7 mm H/X low gamma NMR probe for stationary samples with a dual resonator design.

Quadrupolar echo experiments of the form $\pi/2$-τ-$\pi/2$-acquire were employed for the majority of samples. For **8**, a WURST-QCPMG[5b] sequence, consisting of a WURST-80 pulse followed by a series of refocusing pulses was employed. This sequence was also attempted for compound **2**, however, due to the relatively narrow spectrum and a short T_2 relaxation time, it did not provide signal enhancement. Complete acquisition parameters are given in Table S1.

^{13}C SSNMR spectra were acquired on a Varian Infinity 400 MHz spectrometer. Experimental setup and pulse calibrations were performed on adamantane. Magic-angle spinning (MAS) experiments were performed on a Varian 4 mm HXY probe. Cross polarization experiments were utilized for all compounds. Signals were assigned using solution-state Heteronuclear Multiple Bond Correlation (HMBC) and Heteronuclear Single Quantum Correlation (HSQC) experiments performed on a Varian Inova 400 MHz spectrometer on samples dissolved in C_6D_6.

NMR Spectral Simulations

Experimental NMR parameters were determined from analytical simulations using WSolids.[35] Errors were determined by visual comparison to the experimental spectrum. Starting from the best fit value, the parameter being evaluated was varied systematically in both directions while all others were held constant until a visible change was observed.

Theoretical Calculations

First principles calculations were performed using Gaussian 09[23] on the Shared Hierarchical Academic Research Computing Network (SHARCNET, www.sharcnet.ca). Calculations were performed on a 4 core Opteron 2.4 GHz CPU with 32 GB memory or an 8 core Xeon 2.83 GHz CPU with 16 GB memory. CSA tensors were computed using the gauge-including atomic orbitals (GIAO) method. Basis sets and methods were used as indicated in the results and

discussion. As there is no absolute shielding scale known for germanium, isotropic shifts were calculated relative to $Ge(CH_3)_4$ optimized at the TPSSTPSS[25]/6-31G* level and calculated at the TPSSTPSS/6-311+G** level. The results of the Gaussian calculations were analyzed using EFGShield.[36]

Single Crystal X-ray Diffraction

Data were collected at low temperature (150 K) on a Nonius Kappa-CCD area detector diffractometer with COLLECT. Data were corrected for absorption effects using the multi-scan method (ShADABS). The unit cell parameters were calculated and refined from the full data set.

The structure was solved and refined using the Bruker SHELXTL software package. Subsequent difference Fourier syntheses allowed the remaining atoms to be located. All of the non-hydrogen atoms were refined with anisotropic thermal parameters. Crystallographic data are summarized in Table S2. CCDC-822868 contains the supplementary crystallographic information. These data can be obtained free of charge from The Cambridge Crystallographic Data Center via www.ccdc.cam.ac.uk/data_request/cif.

Acknowledgements

Access to the 900 MHz NMR spectrometer was provided by the *National Ultrahigh-Field NMR Facility for Solids* (Ottawa, Canada), a national research facility funded by the Canada Foundation for Innovation, the Ontario Innovation Trust, Recherche Québec, the National Research Council Canada, and Bruker BioSpin and managed by the University of Ottawa (www.nmr900.ca). Computational work was made possible by the facilities of the Shared Hierarchical Academic Research Computing Network (SHARCNET:www.sharcnet.ca) and Compute/Calcul Canada. We thank Dr. Guerman Popov for the X-ray structure of Ge(*p*-MeO-

$C_6H_4)_4$. The Natural Sciences and Engineering Research Council of Canada (NSERC) is acknowledged for a Major Resources Support grant as well as Discovery Grants to YH and KMB. YH also thanks Canada Research Chair program for funding. We thank Teck Metals Ltd. for a generous donation of $GeCl_4$.

Supporting information for this article is available. Three tables and six figures.

[1] B. Wrackmeyer, *Annu. Rep. NMR Spectrosc.* **2006**, *57*, 1-49.

[2] a) E. Liepins, I. Zicmane, E. Lukevics, *J. Organomet. Chem.* **1988**, *341*, 315-388; b) Y. Takeuchi, T. Takayama, *Annu. Rep. NMR Spectrosc.* **2005**, *54*, 155-200.

[3] P. Pykko, *Mol. Phys.* **2008**, *106*, 1965-1974.

[4] F. H. Larsen, H. J. Jakobsen, P. D. Ellis, N. C. Nielsen, *J. Phys. Chem. A* **1997**, *101*, 8597-8606.

[5] a) R. W. Schurko, I. Hung, C. M. Widdifield, *Chem. Phys. Lett.* **2003**, *379*, 1-10; b) L. A. O'Dell, R. W. Schurko, *Chem. Phys. Lett.* **2008**, *464*, 97-102; c) R. Siegel, T. T. Nakashima, R. E. Wasylishen, *J. Magn. Reson.* **2007**, *184*, 85-100.

[6] S. V. Verkhovskii, A. Y. Yakubovskii, A. Trokiner, B. Z. Malkin, S. K. Saikin, V. I. Ozhogin, A. V. Tikhomirov, A. V. Ananyever, A. P. Gerashenko, Y. V. Piskunov, *Appl. Magn. Reson.* **19**, *17*, 557-576.

[7] Y. Takeuchi, M. Nishikawa, K. Tanaka, T. Takayama, M. Imanari, K. Deguchi, T. Fujito, Y. Sugisaka, *Chem. Commun.* **2000**, 687-688.

[8] Y. Takeuchi, M. Nishikawa, H. Yamamoto, *Magn. Reson. Chem.* **2004**, *42*, 907-909.

[9] Y. Takeuchi, M. Nishikawa, H. Hachiya, H. Yamamoto, *Magn. Reson. Chem.* **2005**, *43*, 662-664.

[10] J. F. Stebbins, L.-S. Du, S. Kroeker, P. Neuhoff, D. Rice, J. Frye, H. J. Jakobsen, *Solid State Nucl. Magn. Reson.* **2002**, *21*, 105-115.

[11] V. K. Michaelis, P. M. Aguiar, V. V. Terskikh, S. Kroeker, *Chem. Commun.* **2009**, 4660-4662.

[12] V. K. Michaelis, S. Kroeker, *J. Phys. Chem. C* **2010**, *114*, 21736-21744.

[13] S. Sen, Z. Gan, *J. Non-Cryst. Solids* **2010**, *356*, 1519-1529.

[14] B. J. Greer, V. K. Michaelis, V. V. Terskikh, S. Kroeker, *Can. J. Chem.* **2011**, *89*, 1118-1129.

[15] A. Sutrisno, M. A. Hanson, P. A. Rupar, V. V. Terskikh, K. M. Baines, Y. Huang, *Chem. Commun.* **2010**, *46*, 2817-2819.

[16] M. Charissé, S. Roller, M. Dräger, *J. Organomet. Chem.* **1992**, *427*, 23-31.

[17] J. B. Lambert, C. L. Stern, Y. Zhao, W. C. Tse, C. E. Shawl, K. T. Lentz, L. Kania, *J. Organomet. Chem.* **1998**, *568*, 21-31.

[18] R. K. Harris, R. E. Wasylishen, M. J. Duer, in *EMR Handbooks*, Wiley, Chichester, UK, **2009**.

[19] C. H. Yoder, T. M. Agee, A. K. Griffith, C. D. J. Schaeffer, M. J. Carroll, A. S. DeToma, A. J. Fleisher, C. J. Gettel, A. L. Rheingold, *Organometallics* **2010**, *29*, 582-590.

[20] G. Ferguson, C. Glidewell, *Acta Crystallogr., Sect. C: Cryst. Struct. Commun.* **1996**, *52*, 1889-1891.

[21] M. Kibalchenko, J. R. Yates, A. Pasquerello, *J. Phys.: Condens. Matter* **2010**, *22*, 145501.

[22] T. Charpentier, *Solid State Nucl. Magn. Reson.* **2011**, *40*, 1-20.

[23] Gaussian 09, Revision A1, M. J. Frisch, Gaussian Inc., Wallingford, CT, 2009

[24] P. J. Stephens, F. J. Devlin, C. F. Chabalowski, M. J. Frisch, *J. Phys. Chem.* **1994**, *98*, 11623-11627.

[25] J. Tao, J. P. Perdew, V. N. Staroverov, G. E. Scuseria, *Phys. Rev. Lett.* **2003**, *91*, 146401.

[26] C. Adamo, V. Barone, *J. Chem. Phys.* **1999**, *110*, 6158-6169.

[27] K. Robinson, G. V. Gibbs, P. H. Ribbe, *Science* **1970**, *172*, 567-570.

[28] S. Freitag, R. Herbst-Immer, L. Lamery, D. Stalke, *Organometallics* **1996**, *15*, 2839-2841.

[29] A. E. Aliev, K. D. M. Harris, D. C. Apperley, *J. Chem. Soc., Chem. Commun.* **1993**, 251-253.

[30] F. Glockling, K. A. Hooton, *J. Chem. Soc.* **1962**, 3509-2512.

[31] D. C. Bradley, L. J. Kay, W. Wardlaw, *J. Chem. Soc.* **1953**, *746*, 4916-4926.

[32] A. G. Brook, F. Abdesaken, H. J. Söllradl, *J. Organomet. Chem.* **1986**, *299*, 9-13.

[33] J. A. Cooke, C. E. Dixon, M. R. Netherton, G. M. Kollegger, K. M. Baines, *Synth. React. Inorg. Met. -Org. Chem.* **1996**, *26*, 1205-1217.

[34] W. Ando, T. Tsumuraya, *Organometallics* **1989**, *8*, 1467-1472.

[35] WSolids1: Solid-State NMR Spectrum Simulation, K. Eichele, R. E. Wasylishen, 2001

[36] S. Adiga, D. Aebi, D. L. Bryce, *Can. J. Chem.* **2007**, *85*, 496-505.

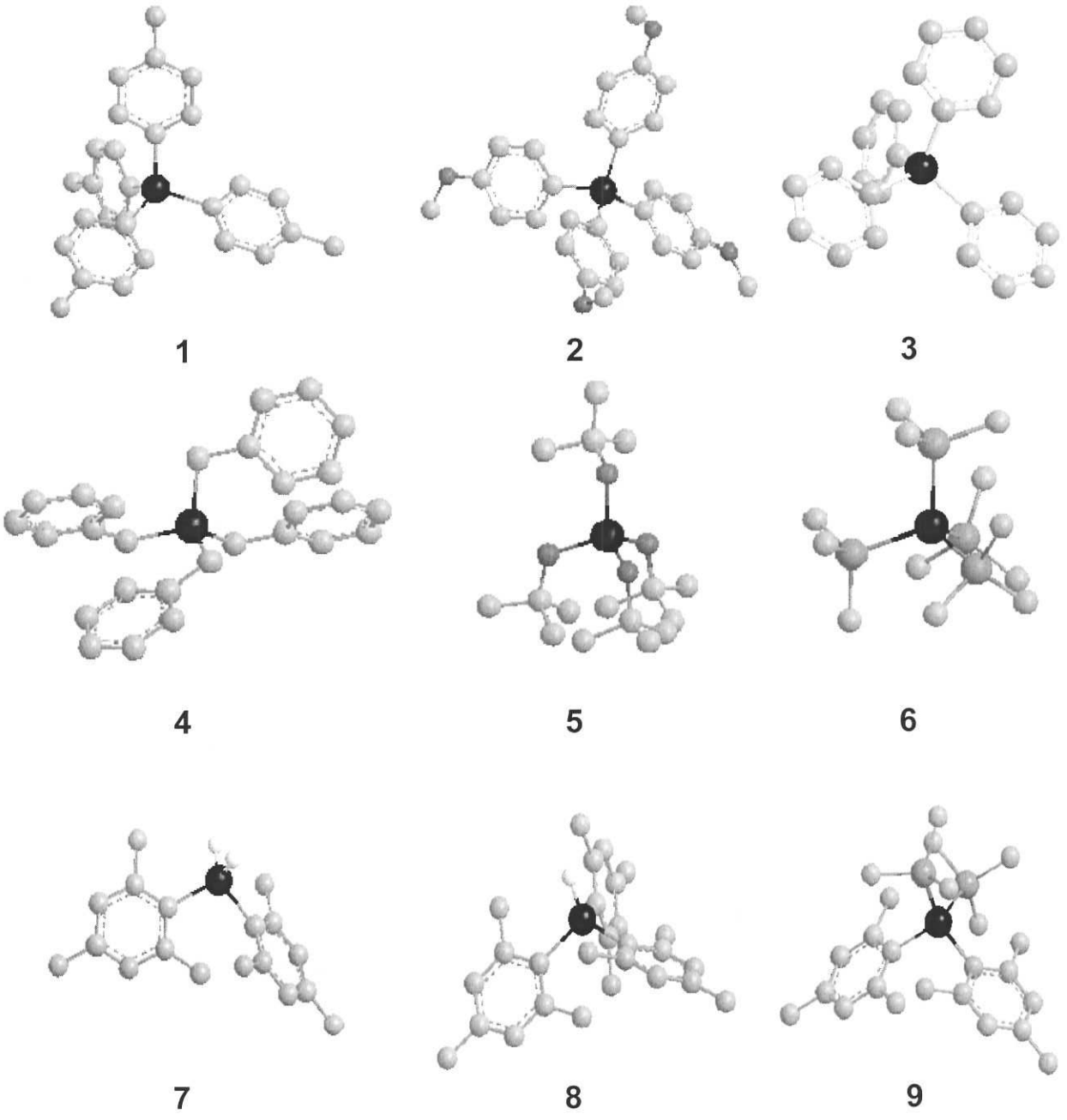

Figure 1: Germanes examined in this study. Hydrogen atoms not directly bound to germanium have been omitted for clarity. **1**) Ge(*p*-Me-C_6H_4)$_4$ **2**) Ge(*p*-OMe-C_6H_4)$_4$ **3**) tetraphenylgermane ($GePh_4$) **4**) tetrabenzylgermane (Ge(CH_2Ph)$_4$) **5**) tetra(*tert*-butoxy)germane (Ge(O*t*Bu)$_4$) **6**) tetrakis(trimethylsilyl)germane (Ge($SiMe_3$)$_4$ **7**) dimesitylgermane (Mes_2GeH_2) **8**) trimesitylgermane (Mes_3GeH) **9**) bis(trimethylsily)dimesitylgermane ($Mes_2Ge(SiMe_3)_2$)

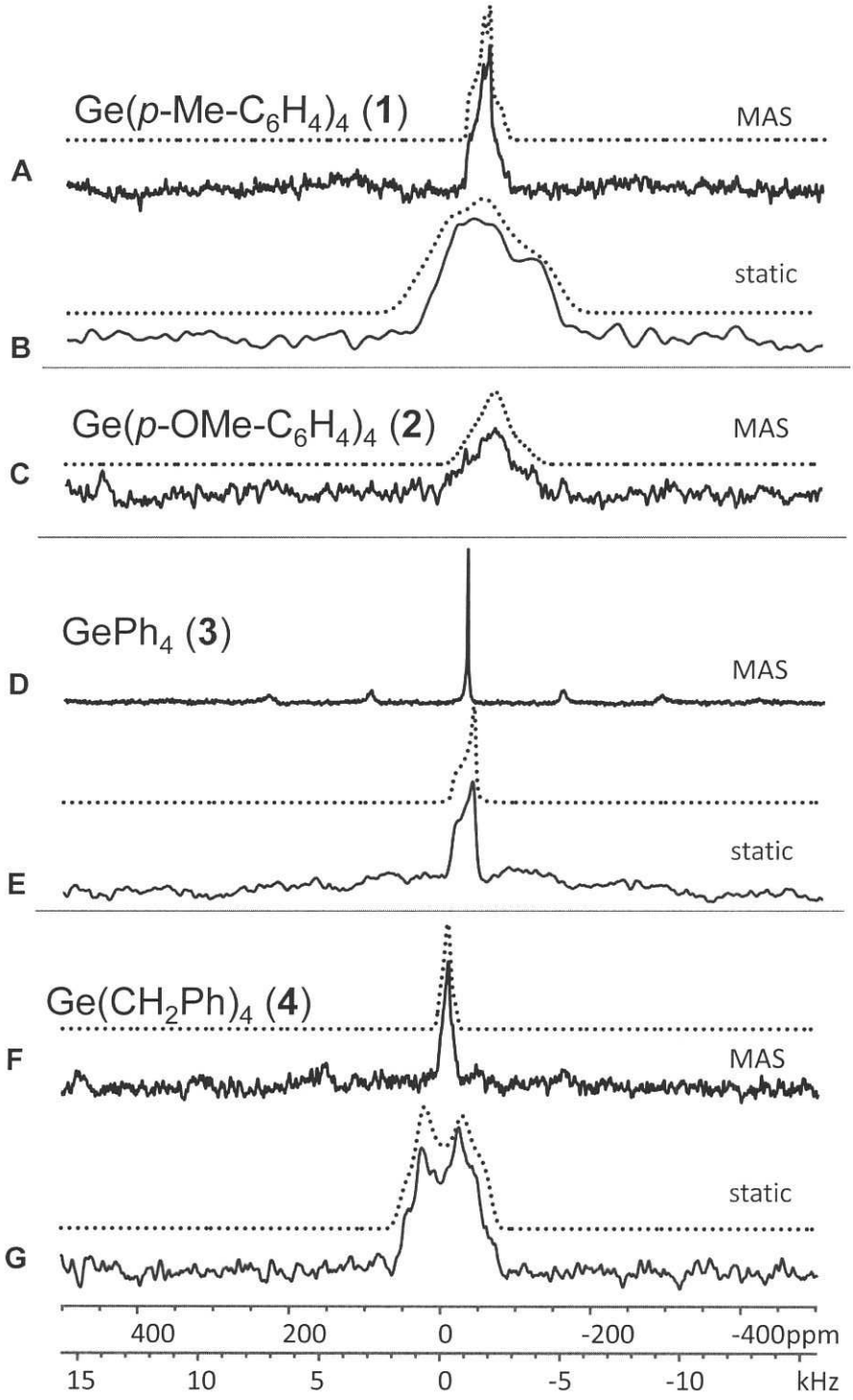

Figure 2: ^{73}Ge SSNMR spectra of compounds **1-4.** Dotted traces represent simulations using parameters from Table 1. A) MAS (5 kHz) and B) static spectra of Ge(p-Me-C_6H_5)$_4$. C) MAS (5 kHz) spectrum of Ge(p-OMe-C_6H_5)$_4$. D) MAS (4 kHz) and E) static spectra of $GePh_4$. F) MAS (5 kHz) and G) static spectra of Ge(CH_2Ph)$_4$.

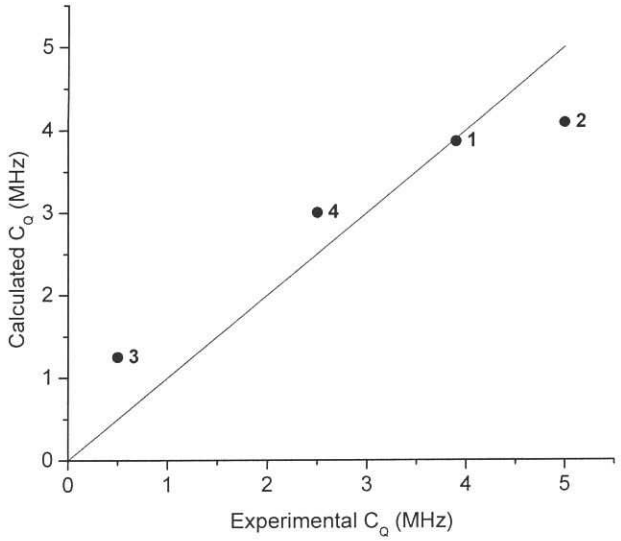

Figure 3: Relationship between experimental and calculated values of C_Q (^{73}Ge)for compounds **1-4.** The solid line represents the ideal 1:1 correlation between experiment and theory. Hydrogen positions were optimized at the TPSSTPSS/6-31G* level.

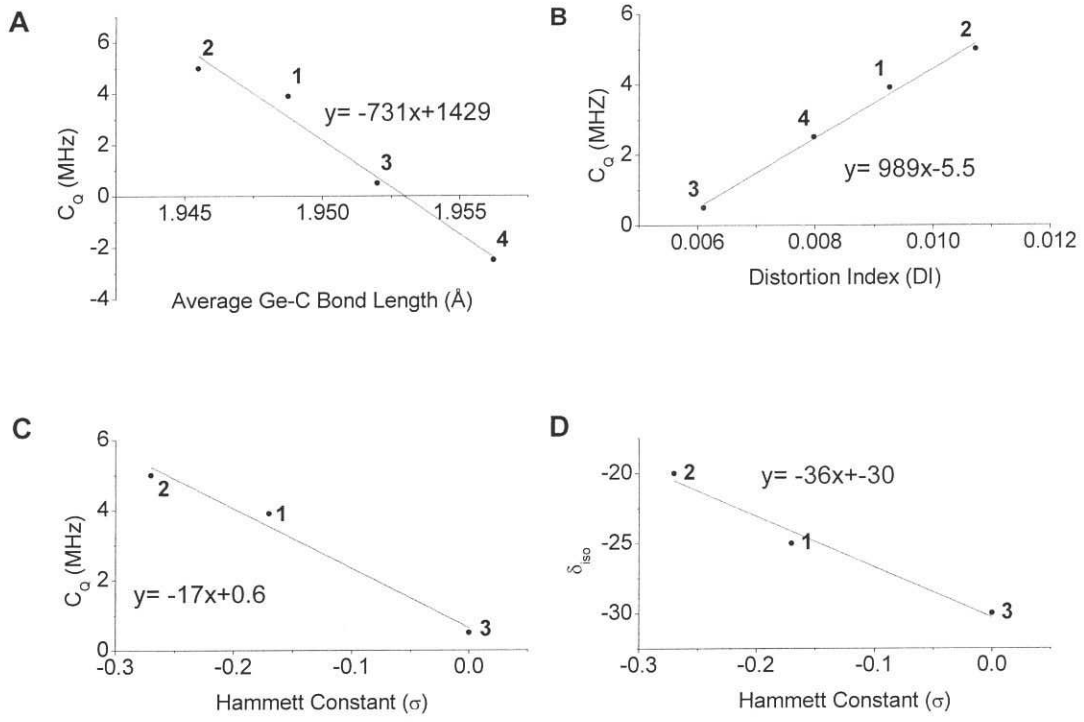

Figure 4: Relationship between A) experimental C_Q and average Ge–C bond length. The sign of C_Q was assumed to be the same as the calculated value. B) experimental C_Q and angular distortion C) experimental C_Q and Hammett constants D) isotropic shift and Hammett constants

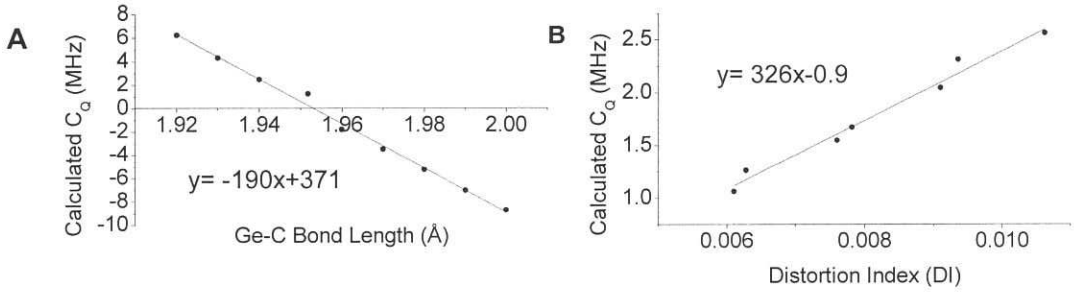

Figure 5: Relationship between A) calculated C_Q and Ge–C bond length and B) calculated C_Q and angular distortion. All calculations were performed at the TPSSTPSS/6-311+G** level.

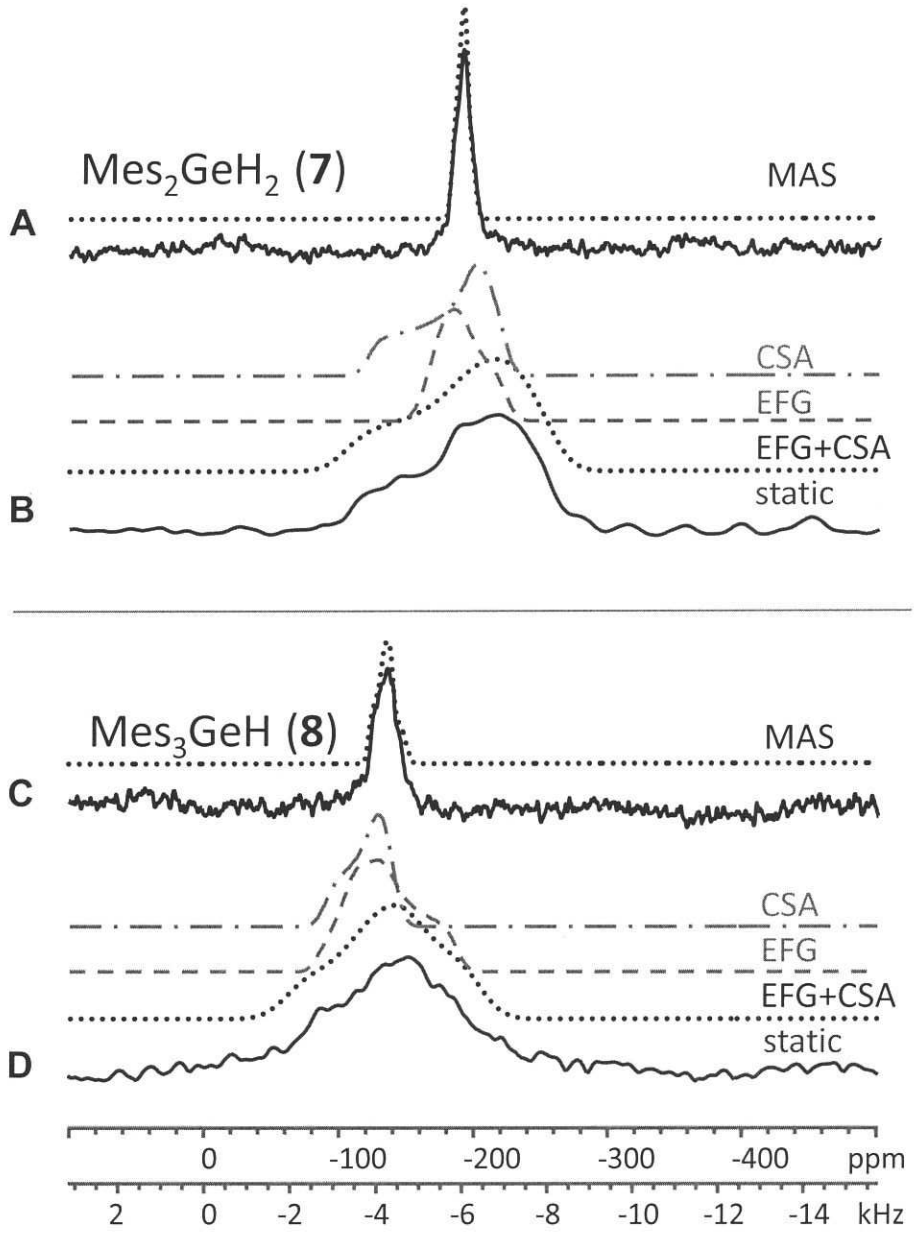

Figure 6: ^{73}Ge SSNMR spectra of compounds **7** and **8.** Dotted traces represent simulations using parameters from Table 1 as discussed in the text. Dashed traces show the individual contributions to the total simulation. A) MAS (5 kHz) and B) static spectra of Mes_2GeH_2. C) MAS (5 kHz) and D) static spectra of Mes_3GeH.

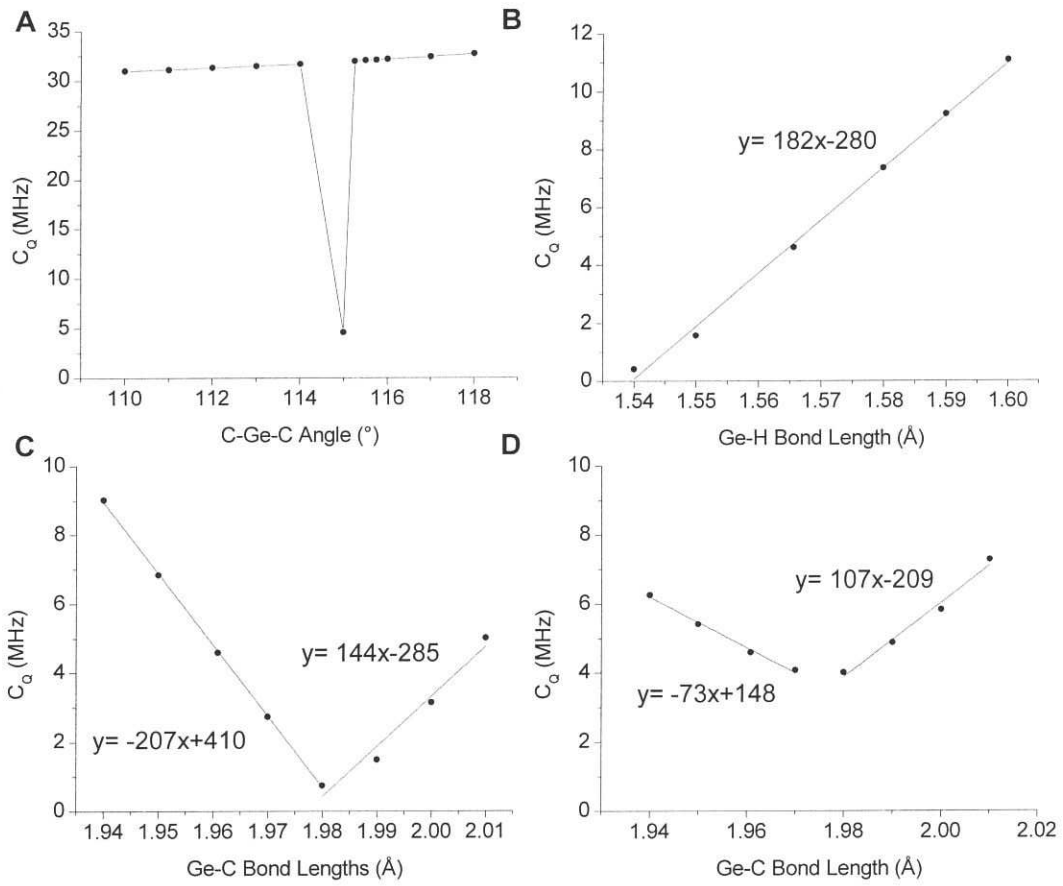

Figure 7: Relationship between calculated C_Q value for Mes_3GeH and A) C–Ge–C bond angle. The geometry optimized value is a notable outlier. B) Ge–H bond length C) all Ge–C bond lengths D) one Ge–C bond length with the others held at their optimized value.

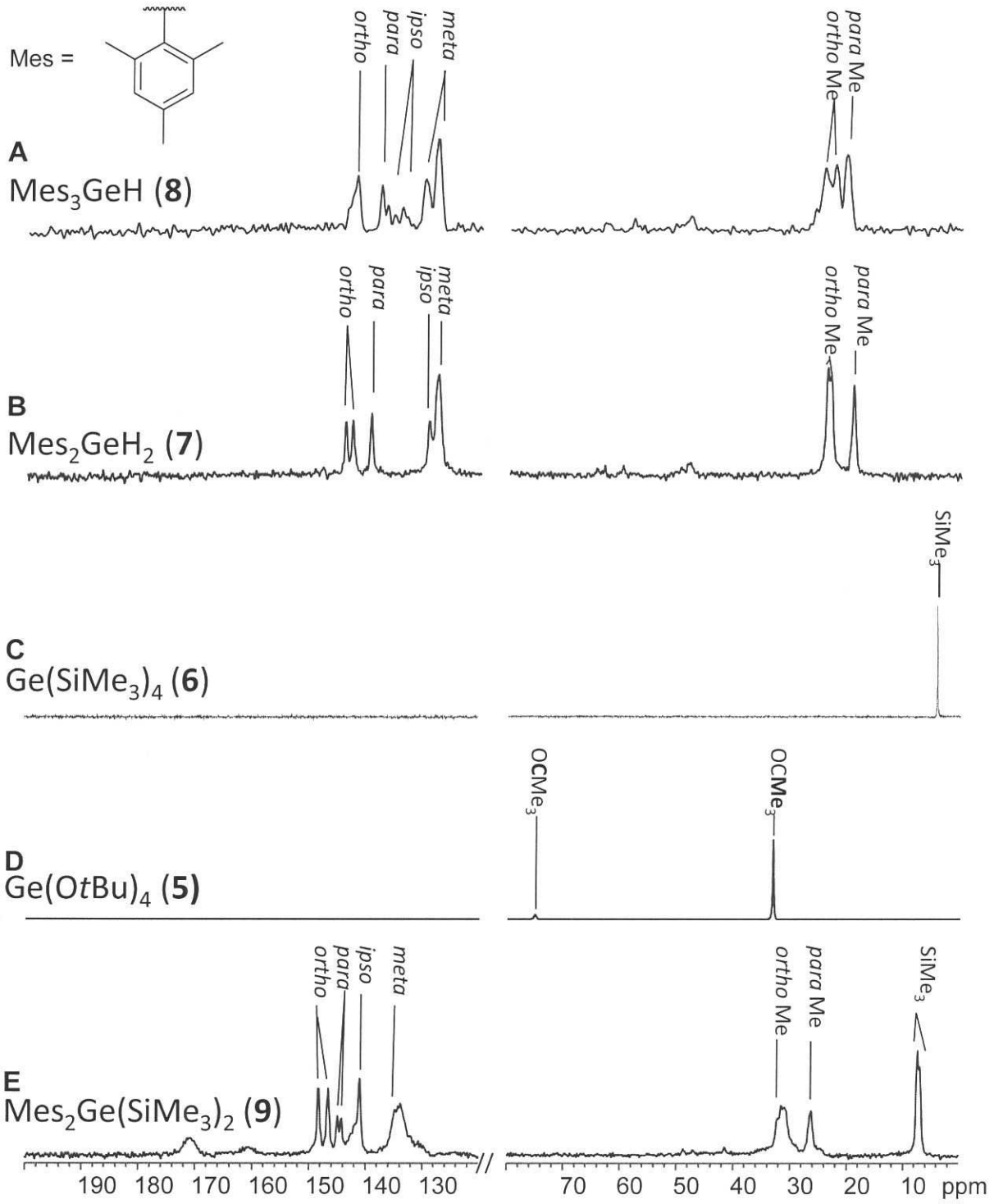

Figure 8: Selected ^{13}C CPMAS SSNMR spectra. A) Mes_3GeH B) Mes_2GeH_2 C) $Ge(SiMe_3)_4$ D) $Ge(OtBu)_4$ E) $Mes_2Ge(SiMe_3)_2$ MAS spinning speed was 8 kHz in A, B and C and 10 kHz in D and E.

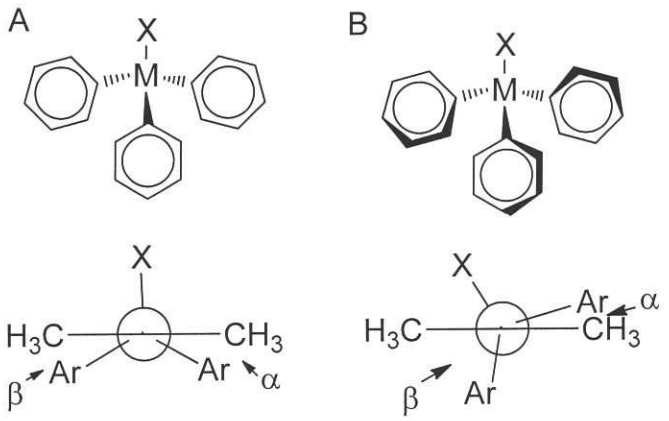

Figure 9: A) The stereographic structure of an untwisted metallane is shown above and its Newman projection below. B) In order to minimize interactions between ortho substituents, the aryl rings twist into a propeller geometry as shown above. The Newman projection below demonstrates the effect of this twisting on the dihedral angles α and β.

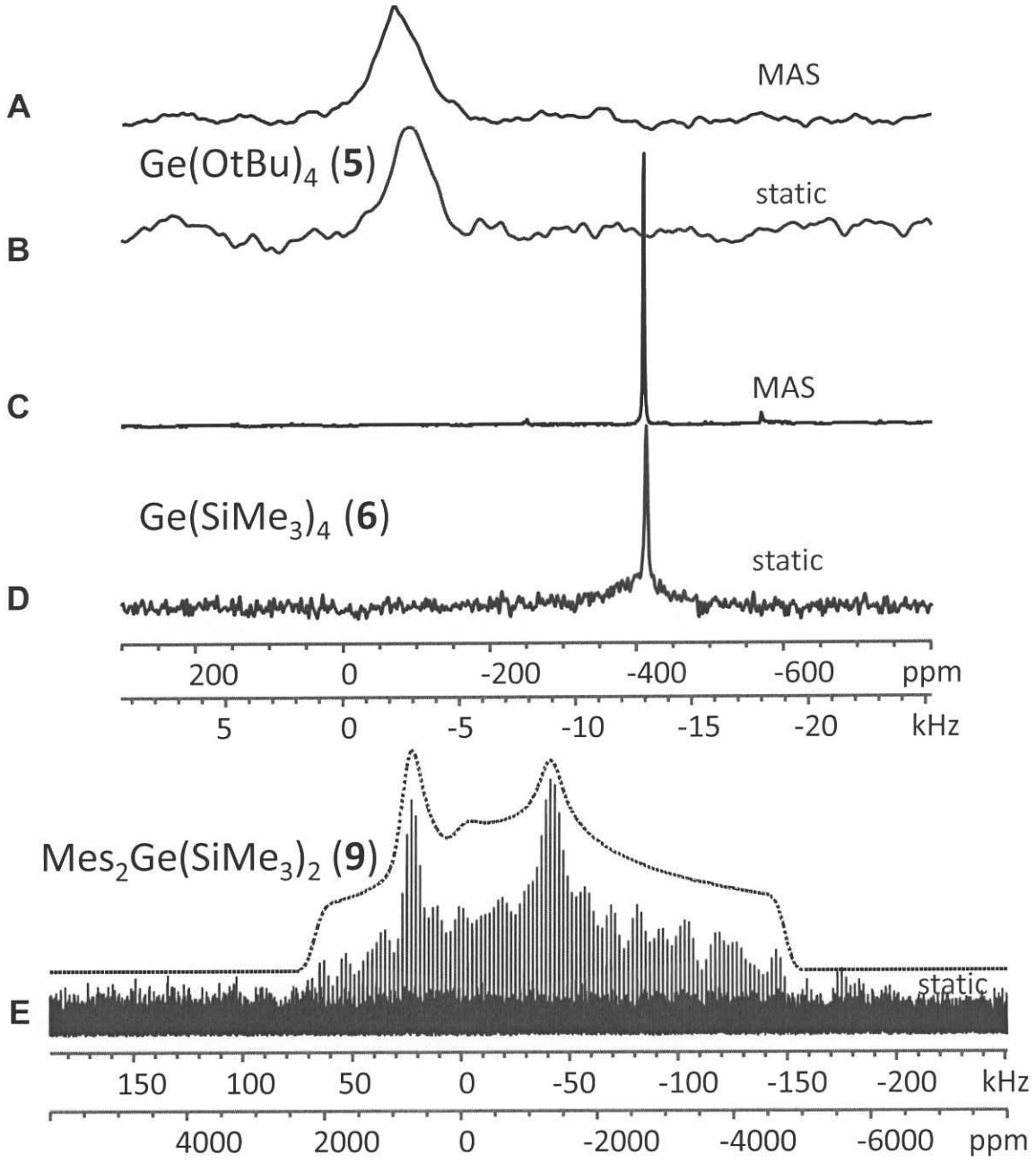

Figure 10: ^{73}Ge SSNMR spectra of compounds **5**, **6** and **9.** Dotted traces represent simulations using parameters from Table 1. A) MAS (5 kHz) and B) static spectra of Ge(O*t*Bu)$_4$. C) MAS (5 kHz) and D) static spectra of $Ge(SiMe_3)_4$. E) Static WURST-CPMG spectrum of $Mes_2Ge(SiMe_3)_2$.

*Table 1. Summary of ^{73}Ge NMR spectroscopic and computational data for compounds **1-9**. In all simulations, the Euler angles $\alpha=\beta=\gamma=0$.*

Structure		**δ_{iso} (ppm)**	**δ solution (ppm)**	**C_Q [a] (MHz)**	**η_Q [b]**	**Ω [c] (ppm)**	**κ [d]**
Ge(*p*-Me-C_6H_4)$_4$ (**1**)	Experimental	-25(5)	-32.4[9]	3.9(2)	0.7(1)	30(10)	0.2(2)
	X-ray[e]	-50		3.7	0.8	35	-0.3
	Optimized [f]	-50		3.9	0	12	-1
Ge(*p*-MeO-C_6H_4)$_4$ (**2**)	Experimental	-20(10)	-11.3[9]	5.0(4)	0.9(2)	n.o.[h]	n.o.[h]
	X-ray [e]	-53	-27.1[19]	3.0	0.7	n. a.[i]	n. a.[i]
	Optimized[f]	-48		4.1	0.1	n. a.[i]	n. a.[i]
$GePh_4$ (**3**)	Experimental	-30(1)	-31.6[9]	0.5	0	30(3)	-1
	X-ray[e]	-55		1.2	0	49	-1
	Optimized[f]	-50		3.8	0	14	-1
Ge(CH_2Ph)$_4$ (**4**)	Experimental	4.5(10)	–	2.5(2)	1.0(1)	60(10)	0.9(1)
	X-ray [e]	-5		-4.1	0.4	59	0.6
	Optimized [f]	-11		-3.0	0.1	89	0.9
Ge($OtBu$)$_4$ (**5**)	Experimental	≈ 0	–	n.a.[i]	-82(1)	≈ 0	n.a.[i]
Ge($SiMe_3$)$_4$ (**6**)	Experimental	≈ 0	–	n.a.[i]	-409(1)	≈ 0	n.a.[i]
Mes_2GeH_2 (**7**)	Experimental	-181(5)	–	2.3(1)	0.7(1)	100(10)	-0.6(1)
	Optimized[f]	-224		5.4	0.1	127	-0.2
	Iterative[g]	-223		0.9	0.6	124	-0.1

Mes_3GeH (**8**)	Experimental	-120(5)	–	2.9(2)	0.7(1)	50(10)	-0.6(1)
	Optimized[f]	-165		-4.6	0	116	-1
	Iterative [g]	-166		3.1	0	116	-1
$Mes_2Ge(SiMe_3)_2$(**9**)	Experimental	-173(1)	–	24.7(3)	0.6(1)	n.o.[h]	n.o.[h]
	Optimized[f]	-204		-19.0	0.5	n. a.[i]	n. a.[i]
	Iterative[g]	-205		-24.5	0.5	n. a.[i]	n. a.[i]

[a] $C_Q = (eV_{ZZ}Q/h)$ (Quadrupolar coupling constant) [b] $\eta_Q = (V_{XX} - V_{YY})/V_{ZZ}$ (Quadrupolar asymmetry parameter) [c] $\Omega = \delta_{11} - \delta_{33}$ (CSA span) [d] $\kappa = 3(\delta_{22} - \delta_{iso})/\Omega$ (CSA skew) [e] Calculated parameters using crystallographically determined geometry (hydrogen positions optimized at the TPSSTPSS/6-31G* level) [f] Calculated parameters using structure optimized at the TPSSTPSS/6-31G* level [g] Calculated parameters using geometry obtained by systematic variation of structural metrics [h] n.o.= not observed [i]n.a.= not applicable

Table 2. Summary of computational results for ***1*** *using different model chemistries*

Entry	Method	Basis Set	C_Q (MHz)	η	Ω (ppm)	κ
1	HF	6-31G*	2.2	0.5	67	0.7
2	B3LYP	6-31G*	2.3	0.9	76	0.6
3	PBE1PBE	6-31G*	2.2	0.9	76	0.6
4	TPSSTPSS	6-31G*	2.4	0.8	76	0.6
5	HF	6-311+G**	4.5	0.7	32	-0.2
6	B3LYP	6-311+G**	3.9	0.8	36	-0.3
7	PBE1PBE	6-311+G**	3.9	0.8	35	-0.3
8	TPSSTPSS	6-311+G**	3.7	0.7	35	-0.3
9	Experimental		3.9(2)	0.7(1)	30(10)	0.2(2)

ELECTRONIC SUPPORTING INFORMATION for

Solid-State ^{73}Ge NMR Spectroscopy of Simple Organogermanes

Margaret A. Hanson, Andre Sutrisno, Victor V. Terskikh, Kim M. Baines*, Yining Huang*

Table S1. Detailed ^{73}Ge SSNMR experimental conditions.

Sample	Type of experiment	pulse length (μs)	SW (kHz)	recycle delay (s)	τ_1 (μs)	# scans
Ge(*p*-Me-C_6H_4)$_4$	MAS 5 kHz	4.0	50	2	---	27132
	static echo	4.0	250	2	19.6	25440
Ge(*p*-MeO-C_6H_4)$_4$	MAS 5 kHz	4.0	50	2	---	31512
$GePh_4$	MAS 4 kHz	3.0	500	1	---	1024
	static echo	3.0	100	5	19.6	10237
Ge(CH_2Ph)$_4$	MAS 5 kHz	4.0	100	1	---	37833
	static echo	4.0	200	1	19.6	71680
Ge(O*t*Bu)$_4$	MAS 5 kHz	4.0	100	1	---	10240
	static echo	4.0	200	1	19.6	64679
Ge($SiMe_3$)$_4$	MAS 5 kHz	4.0	50	1	---	256
	static echo	4.0	250	1	19.6	14000
Mes_2GeH_2	MAS 5 kHz	4.0	50	2	---	2500
	static echo	4.0	250	2	19.6	29131
Mes3GeH	MAS 5 kHz	4.0	50	2	---	2403
	static echo	4.0	250	2	19.6	40360
$Mes_2Ge(SiMe_3)_2$	static WURST-QCPMG*	50	500	1	25	131639

* τ_a= 132 μs, M (# of loops)=64, τ_2= 26 μs, τ_3= 26 μs, τ_4= 26 μs

Table S2. Crystallographic data for Ge(p-MeO-C_6H_4)$_4$.

empirical formula	$C_{28}H_{28}GeO_4$
fw	501.09
cryst syst	triclinic
space group	P-1
a (Å)	10.525(2)
b (Å)	10.973(2)
c (Å)	11.939(2
α (deg)	70.916(4)
β (deg)	69.605(4)
γ (deg)	77.627(4)
volume (Å^3)	1213.5(4)
Z	2
no. of data/restraints/params	5487 / 0 / 302
goodness-of-fit	1.005
R [$I > 2\sigma(I)$]	0.0475
wR^2 (all data)	0.0823
largest diff peak and hole (e Å^{-3})	0.498, -0.504

Table S3. Selected crystallographic bond lengths and angles for Ge(p-MeO-C_6H_4)$_4$.

Ge–C Bond Lengths (Å)	**C–Ge–C Bond Angles (°)**
1.949(3)	107.4(1)
1.940(4)	111.2(1)
1.943(3)	110.7(1)
1.950(3)	108.3(1)
	109.9(1)
	109.2(1)

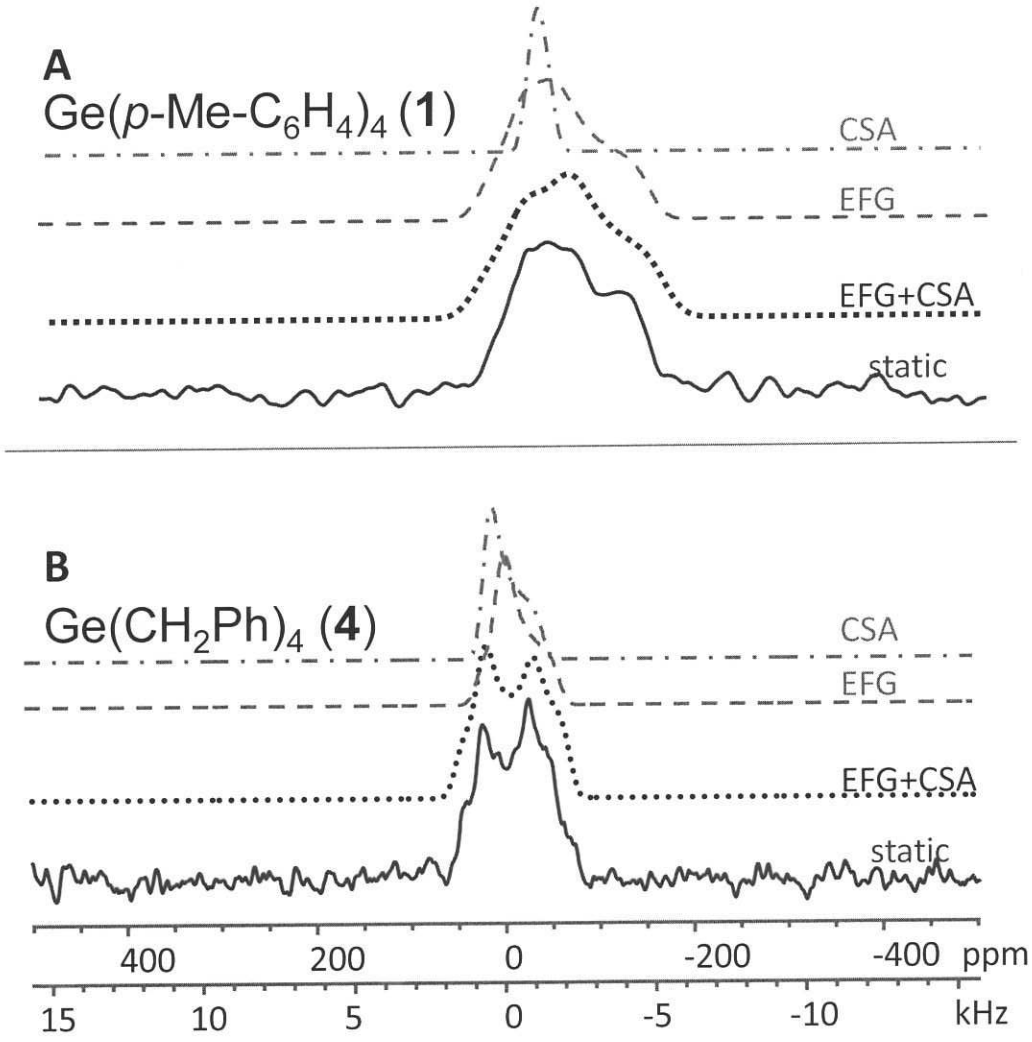

Figure S1. Simulation breakdown of A) Ge(p-MeC_6H_4)$_4$ and B) Ge(CH_2Ph)$_4$ showing the individual contributions of CSA (purple dash-dot line), EFG (red dashed line), and the two combined (black dotted line).

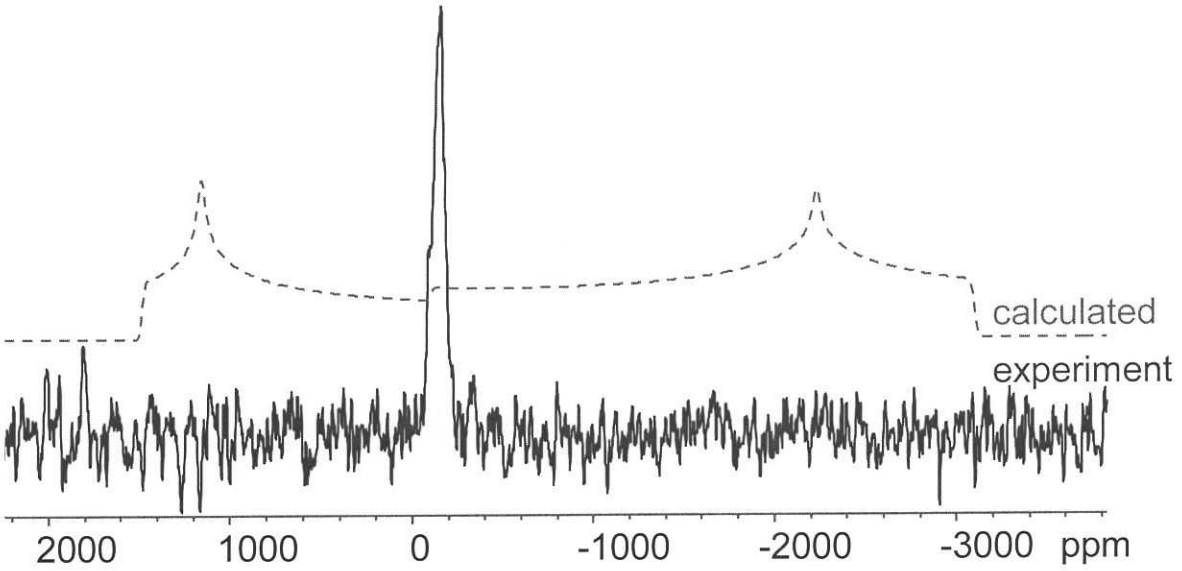

Figure S2. Comparison between experimental spectrum of a stationary sample of Mes_3GeH (blue solid line) and that predicted computationally from the X-ray structure (red dashed line).

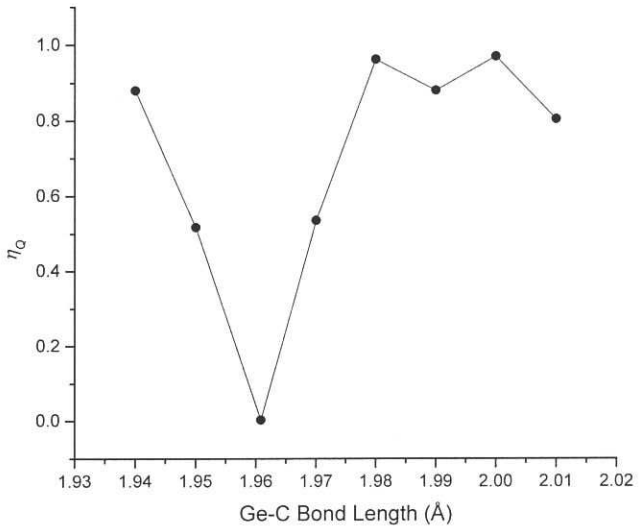

Figure S3. Effect of changing the length of a single Ge-C bond in Mes_3GeH on the calculated value of η_Q.

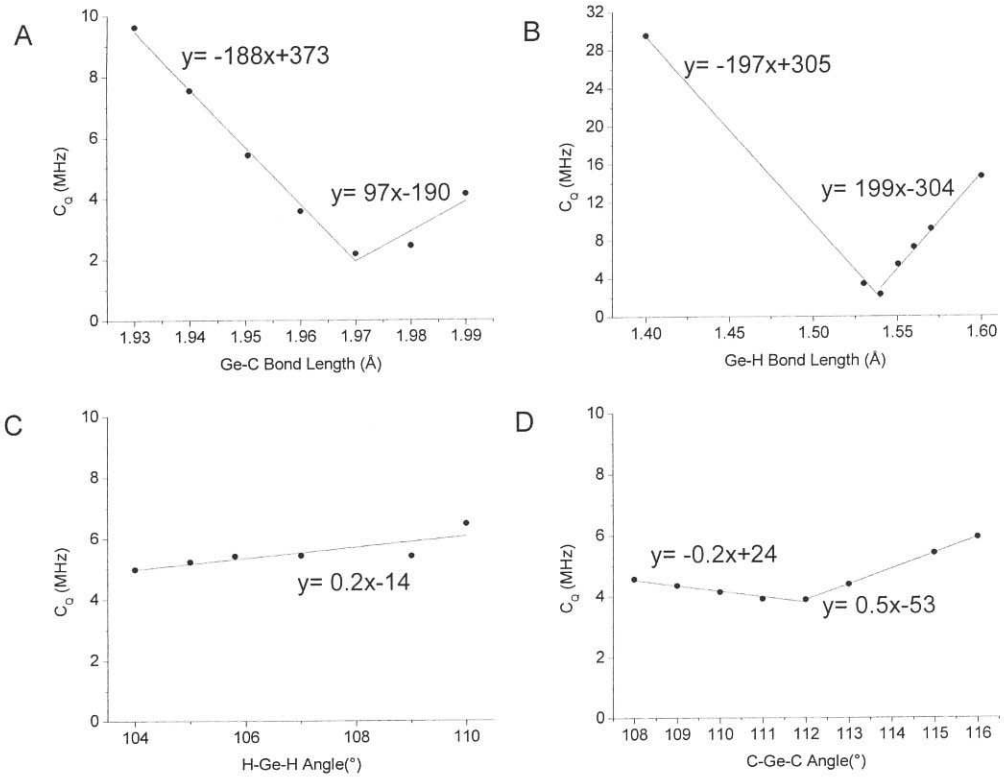

Figure S4. Relationship between the calculated C_Q value for Mes_2GeH_2 and A) Ge–C bond lengths, B) Ge–H bond lengths, C) H–Ge–H bond angle, and D) C–Ge–C bond angle.

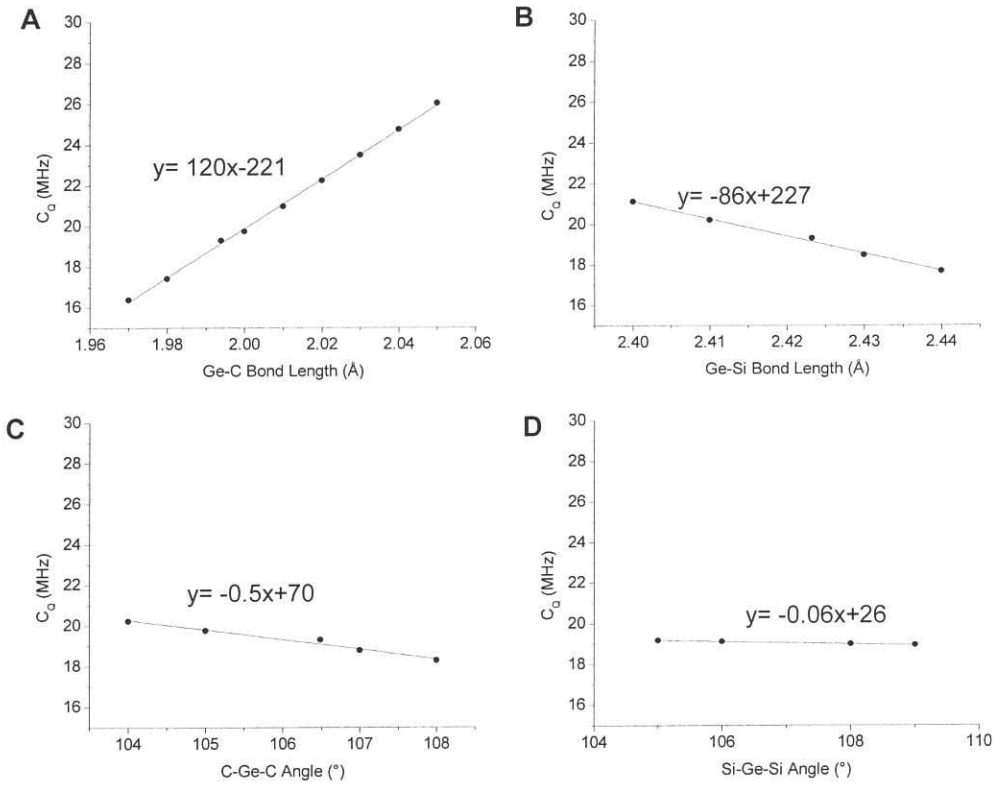

Figure S5. Relationship between the calculated C_Q value for $Mes_2Ge(SiMe_3)_2$ and A) Ge–C bond lengths, B) Ge–Si bond lengths, C) C–Ge–C angle, and D) Si–Ge–Si angle.

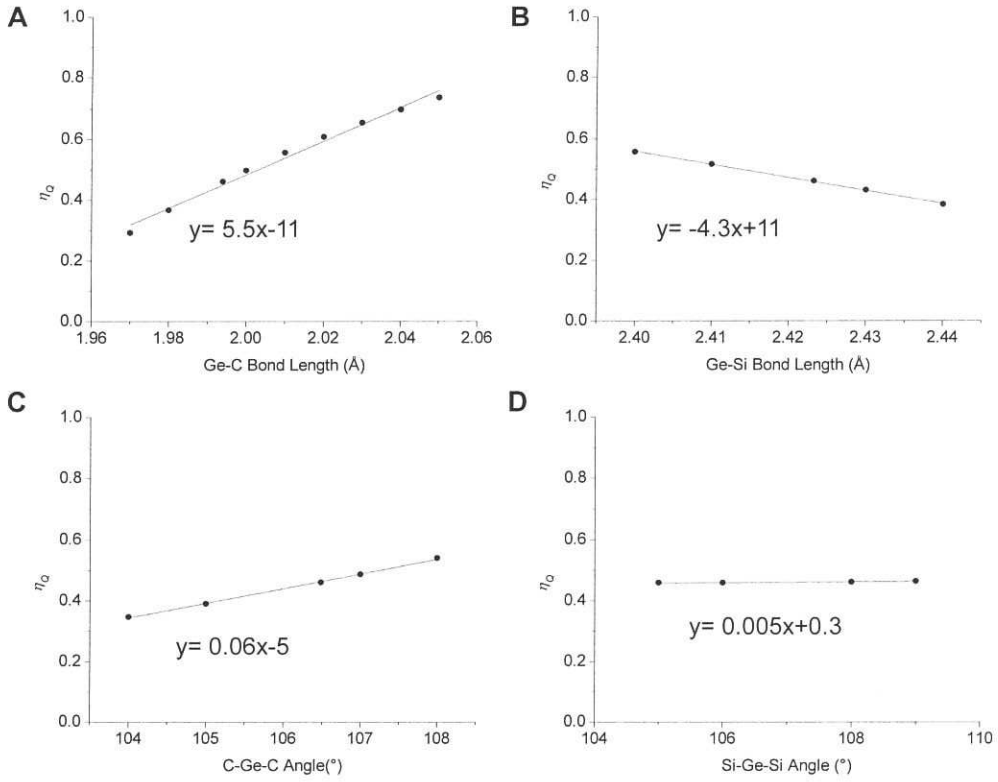

Figure S6. Relationship between the calculated η_Q value for $Mes_2Ge(SiMe_3)_2$ and A) Ge–C bond lengths, B) Ge–Si bond lengths, C) C–Ge–C bond angle, and D) Si–Ge–Si bond angle.